Inorganic Chemistry
Article

Inorg. Chem. **2009**, *48*, 11131–11141 **11131**
DOI: 10.1021/ic901506v

Palladium Motion in Cyclomeric Compounds: A Theoretical Study

Antonio J. Mota*,† and Alain Dedieu‡

†*Departamento de Química Inorgánica, Facultad de Ciencias, Universidad de Granada, Campus de Fuentenueva, 18002-Granada, Spain and* ‡*Laboratoire de Chimie Quantique, Institut de Chimie, UMR 7177 CNRS/UdS Université de Strasbourg, 4, rue Blaise Pascal, 67000 Strasbourg, France*

Received July 29, 2009

Density functional theory (DFT)/B3LYP calculations have been carried out to study successive intramolecular 1,*n* palladium shifts (*n* = 3−5) in palladium complexes of organic cyclomers. Such shifts of the PdBr(phosphine) moiety, which is bound to the cyclomer and which exchanges concomitantly with a hydrogen atom distant by *n* carbon atoms from palladium, might lead to an endless motion around the cyclomer. The cyclomers that have been analyzed are either the [1,1,1,1]paracyclophane **1**, a THF-based 16-crown-4 structure **2**, or the THF-ethylene cyclic dimer **3** (THF = tetrahydrofuran). We show that the [1,1,1,1]paracyclophane **1** is not a good candidate for a circular motion of the metallic moiety. This is due to the very high barrier of the 1,2 Pd/H exchange within the phenyl ring. Hence only a pendulum movement of the metallic moiety between two adjacent phenyl rings can easily take place. For the THF-based systems **2** and **3**, the processes along the *exo* face are found to involve high energy barriers. Processes along the *endo* face are more accessible, especially for **2** where an endless motion made of successive 1,2 and 1,5 shifts is characterized by barriers that are somewhat less than 30 kcal mol^{-1}.

Introduction

There have been recent examples in organopalladium chemistry of palladium displacement reactions along a chain of carbon atoms that are part of palladium-catalyzed multistep transformations.[1−17] These displacement reactions between two carbon atoms, which consist of a forward 1,*n* Pd migration associated to a concomitant backward shift of a hydrogen, are important from a synthetic point of view because they allow in certain instances the attachment of groups in positions that are otherwise difficult to substitute by usual chemical reactions.[17] In the recent past years we have attempted to shed light on the mechanism of such 1,*n* Pd/H exchange through several theoretical studies that focused on the processes of intramolecular nature.[18−20] We were in particular able to delineate the electronic and geometric factors that account for the existence of Pd(II) and/or Pd(IV) transient species (either transition states or intermediates). One of the conclusions reached is that very often pathways corresponding to both oxidation states might operate, in some instances competitively, the geometric constraints being a determinant factor for the preference of one pathway over the other. As shown in Scheme 1, Pd(IV) transitions states and intermediates are favored by a planar arrangement of the two organic moieties with the transferred hydrogen being a hydride sitting more or less at the apex, whereas the Pd(II) transition state is helped by a clamping arrangement of these two organic moieties, the hydrogen being then transferred as a proton and sitting more or less in the plane defined by palladium and the non organic ancillary ligands. These conclusions were found to be valid for various kinds of Pd/H rearrangements, either between two sp^2 carbon atoms or between an sp^2 and an sp^3 carbon atom of the chain.

*To whom correspondence should be addressed. E-mail: mota@ugr.es. Phone: +34 9 58 24 04 42. Fax: +34 9 58 24 85 26.

(1) Wang, L.; Pan, Y.; Jiang, X.; Hu, H. *Tetrahedron Lett*. **2000**, *41*, 725.
(2) Tian, Q.; Larock, R. C. *Org. Lett*. **2000**, *2*, 3329.
(3) Larock, R. C.; Tian, Q. *J. Org. Chem*. **2001**, *66*, 7372.
(4) Karig, G.; Moon, M.-T.; Thasana, N.; Gallagher, T. *Org. Lett*. **2002**, *4*, 3115.
(5) Campo, M. A.; Larock, R. C. *J. Am. Chem. Soc*. **2002**, *124*, 14326.
(6) Campo, M. A.; Huang, Q.; Yao, T.; Tian, Q.; Larock, R. C. *J. Am. Chem. Soc*. **2003**, *125*, 11506.
(7) Huang, Q.; Campo, M. A.; Yao, T.; Tian, Q.; Larock, R. C. *J. Org. Chem*. **2004**, *69*, 8251.
(8) Huang, Q.; Fazio, A.; Dai, G.; Campo, M. A.; Larock, R. C. *J. Am. Chem. Soc*. **2004**, *126*, 7460.
(9) Barder, T. E.; Walker, S. D.; Martinelli, J. R.; Buchwald, S. L. *J. Am. Chem. Soc*. **2005**, *127*, 4685.
(10) Zhao, J.; Larock, R. C. *Org. Lett*. **2005**, *7*, 701.
(11) Zhao, J.; Campo, M.; Larock, R. C. *Angew. Chem., Int. Ed*. **2005**, *44*, 1873.
(12) Bour, C.; Suffert, J. *Org. Lett*. **2005**, *7*, 653.
(13) Masselot, D.; Charmant, J. P. H.; Gallagher, T. *J. Am. Chem. Soc*. **2006**, *128*, 694.
(14) Zhao, J.; Larock, R. C. *J. Org. Chem*. **2006**, *71*, 5340.
(15) Singh, A.; Sharp, P. R. *J. Am. Chem. Soc*. **2006**, *128*, 5998.
(16) Campo, M.; Zhang, H.; Yao, T.; Ibdah, A.; McCulla, R. D.; Huang, Q.; Zhao, J.; Jenks, W. S.; Larock, R. C. *J. Am. Chem. Soc*. **2007**, *129*, 6298.
(17) Ma, S.; Gu, Z. *Angew. Chem., Int. Ed*. **2005**, *44*, 7512.
(18) Mota, A. J.; Dedieu, A.; Bour, C.; Suffert, J. *J. Am. Chem. Soc*. **2005**, *127*, 7171.
(19) Mota, A. J.; Dedieu, A. *Organometallics* **2006**, *25*, 3130.
(20) Mota, A. J.; Dedieu, A. *J. Org. Chem*. **2007**, *72*, 9669.

Published on Web 11/10/2009

Scheme 1. Different Spatial Arrangements for the Intramolecular 1,*n* Pd/H Interchange in Carbo-Palladated Systems

Scheme 2. Organic Scaffolds Used in This Work for the Study of the Palladium Motion

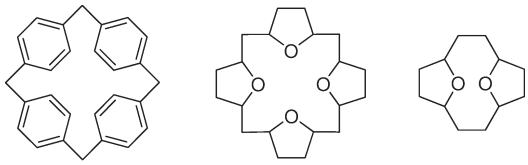

We also analyzed the 1,2 Pd/H rearrangement between two sp^3 carbon atoms, that may be involved in the so-called "chain running" rearrangements.[21−25] It takes place via transition states and intermediates on a relatively flat energy profile.

Extending the scope of our investigations we asked ourselves whether migrations of the type mentioned above could be used for the creation of molecular machines and/or switches. For this purpose, we went from linear chains to cyclomeric systems, where a succession of 1,*n* Pd/H rearrangements (with various *n* values) could lead to an endless motion around the organic cycle. We report here the results of a theoretical investigation on systems that might be good candidates for having this property. The systems under study are monopalladated bromo systems that would chemically result from an initial oxidative addition of a palladium(0) phosphine complex to the C−Br bond of the corresponding monobromated derivative of either [1,1,1,1]paracyclophane **1**, a THF-based 16-crown-4 structure **2**, or the THF-ethylene cyclic dimer **3** (THF = tetrahydrofuran), see Scheme 2, where the most stable conformers have been used in each case.

The starting structures of these cyclomers were obtained from a conformational analysis carried out by means of the molecular mechanics MM+ force field[26] implemented in the Hyperchem 7.52 program.[27] Geometries were subsequently refined through AM1 semiempirical MO calculations[28] to get the better starting candidates.

Computational Details

The calculations were carried out at the DFT-B3LYP level[29−31] with the Gaussian 03 program.[32] The phosphine ligand was modeled by PH_3. The geometries were fully optimized by the gradient technique with the following basis: For Pd the LANL2DZ basis set is modified following the prescription of Couty and Hall.[33] In this modified basis the innermost core electron (up to 3d) are described by the relativistic orbital-adjusted effective core potential of Hay and Wadt,[34] and the remaining outer core and valence electrons by a [341/541/31] basis set where the two outermost 5p functions of the standard LANL2DZ basis set have been replaced by a [41] split of the 5p function optimized by Couty and Hall.[33] For the Br atom the quasi relativistic energy-adjusted spin averaged effective core potential was taken from the work of the Stuttgart group, together with their [31/31] basis set,[35] to which s and p diffuse functions (with exponents of 0.0493 and 0.0363, respectively), and a d polarization function (of exponent 0.381) were added, following Radom et al.[36] The other atoms were described by the standard polarized 6-31G* basis set.[37] Although our first study[18] indicated that the geometrical parameters obtained with this basis set were in agreement with related experimental structures of bromo-palladium complexes and that the thermodynamic values obtained with this basis set were quite comparable to those obtained with larger basis sets, we checked that for energy barriers the use of a larger basis set for these atoms, namely, the 6-311+G(d,p) basis set, would not change the results obtained with the 6-31G* basis set. The corresponding calculations were performed for selected 1,3 Pd migrations, which are characterized by uncommon transition states (vide infra). The *cis*/*trans* label that will be used throughout this paper refers to the relative position of the bromine atom and the carbon atom covalently bound to palladium. Note that a 1,*n* Pd migration will connect a *cis* structure to a *trans* structure, and vice versa, when $n \geq 3$, whereas the geometric configuration is conserved for $n = 2$. The nature of the optimized structures, either transition states or intermediates, was assessed through a frequency calculation. Since we are dealing here with intramolecular processes, we will concentrate on enthalpy values, which were obtained by taking into account the zero-point energies and the thermal motion at standard conditions (temperature of 298.15 K, pressure of 1 atm).

Results

(A). [1,1,1,1]paracyclophane (1). The palladium complex derived from [1,1,1,1]paracyclophane **1**,[38] see Scheme 3, was the system that we first selected. For such

(21) Schmidt, G. F.; Brookhart, M. *J. Am. Chem. Soc.* **1985**, *107*, 1443.
(22) Brookhart, M.; Volpe, A. F.; Lincoln, D. M.; Hovarth, I. T.; Millar, J. M. *J. Am. Chem. Soc.* **1990**, *112*, 5634.
(23) Brookhart, M.; Grant, B. E. *J. Am. Chem. Soc.* **1993**, *115*, 2151.
(24) Rix, F. C.; Brookhart, M.; White, P. S. *J. Am. Chem. Soc.* **1996**, *118*, 2436.
(25) See also: (a) Negishi, E.; Copéret, C.; Ma, S.; Liou, S.-Y.; Liu, F. *Chem. Rev.* **1996**, 365. (b) Herrmann, W. A.; Öfele, K.; Preysing, D. v.; Schneider, S. K. *J. Organometallics* **2003**, *687*, 229. (c) Palladium Chemistry in 2003: Recent Developments, special issue of *J. Organomet. Chem.*; Bertrand, G., Ed.(d) Zeni, G.; Larock, R. C. *Chem. Rev.* **2004**, *104*, 2285. (e) Tietze, L. F.; Ila, H.; Bell, H. P. *Chem. Rev.* **2004**, *104*, 3453. (i) Dupont, J.; Consort, C. S.; Spencer, J. *Chem. Rev.* **2005**, *105*, 2557. (f) Zeni, G.; Larock, R. C. *Chem. Rev.* **2006**, *106*, 4644. (g) Yin, L.; Liebscher, J. *Chem. Rev.* **2007**, 133. (h) Alberico, D.; Scott, M. E.; Lautens, M. *Chem. Rev.* **2007**, 174.
(26) MM+ supplements the standard Allinger's MM2 force field by providing additional parameters. As references see: (a) Allinger, N. L. *J. Am. Chem. Soc.* **1977**, *99*, 8127. (b) Lii, J.; Gallion, S.; Bender, C.; Wikstrom, H.; Allinger, N. L.; Flurchick, K. M.; Teeter, M. M. *J. Comput. Chem.* **1989**, *10*, 503. (c) Hocquet, A; Langgård, M. *J. Mol. Model.* **1998**, *4*, 94.
(27) *Hyperchem 7.52*; Hypercube, Inc.: 1115 NW 4th St., Gainesville, FL 32608, U.S.A.
(28) Dewar, M. J. S.; Zoebisch, E. G.; Healy, E. F.; Stewart, J. P. P. *J. Am. Chem. Soc.* **1985**, *107*, 3902.
(29) Becke, A. D. *Phys. Rev. A* **1988**, *38*, 3098.
(30) Lee, C.; Yang, W.; Parr, R. G. *Phys. Rev. B* **1988**, *37*, 785.
(31) Becke, A. D. *J. Chem. Phys.* **1993**, *98*, 5648.
(32) Frisch, M. J. et al.*Gaussian 03*, Revision B.04; Gaussian, Inc.: Pittsburgh, PA, 2003. See the Supporting Information for the complete reference.
(33) Couty, M.; Hall, M. B. *J. Comput. Chem.* **1996**, *17*, 1359.
(34) Hay, P. J. *J. Chem. Phys.* **1985**, *82*, 299.
(35) Bergner, A.; Dolg, M.; Küchle, W.; Stoll, H.; Preuss, H. *Mol. Phys.* **1993**, *80*, 1431.
(36) Glukhovtsev, M.; Pross, A.; McGrath, M. P.; Radom, L. *J. Chem. Phys.* **1995**, *103*, 1878.
(37) Hehre, W. J.; Ditchfield, R.; Pople, J. A. *J. Chem. Phys.* **1972**, *56*, 2257.
(38) Miyahara, Y.; Inazu, T.; Yoshino, T. *Tetrahedron Lett.* **1983**, *24*, 5277.

Scheme 3. 1,5 Pd/H Interchange in the [1,1,1,1]paracyclophane System

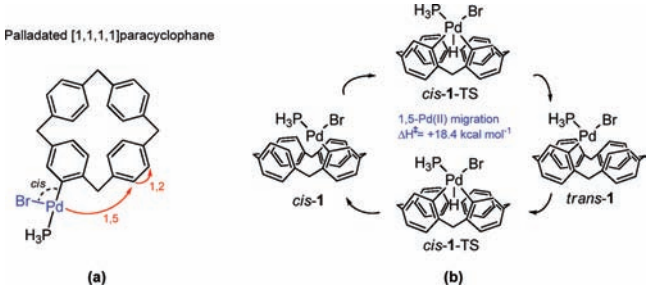

Scheme 4. Simplified Mechanism for the 1,2-Pd Migration Process between Two sp^2 (left) and Two sp^3 Carbon Atoms (right)

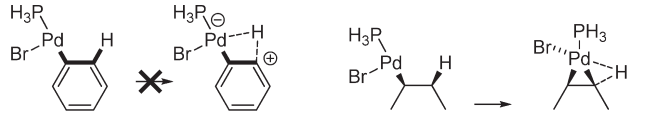

Scheme 5. 1,2 + 1,5 Tandem Pd/H Interchange in the THF-Based 16-crown-4 System **2**: Geometric and Isomeric Considerations

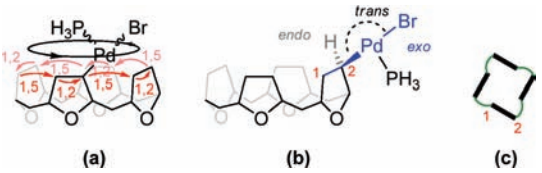

a system one would have expected the $PdBr(PH_3)$ group turning forever around the upper carbon skeleton via [1,5 + 1,2] migration sequences, see (a) in Scheme 3.

But whereas the 1,5-Pd/H rearrangement between two adjacent phenyl groups is an easy process, with a computed enthalpy barrier as low as 18.4 kcal mol^{-1}, the 1,2-Pd/H rearrangement is not possible, since it has to overcome an enthalpy barrier of 52.0 kcal mol^{-1}. This high barrier can be traced to the coplanarity, imposed by the phenyl ring, of the palladium and of the hydrogen that should exchange in the 1,2 process, see Scheme 4.

As a result of this high barrier for the 1,2 process the displacement that one could observe for the palladated [1,1,1,1]paracyclophane, (a) in Scheme 3, would merely consist of a through-space 1,5 oscillating movement of Pd back and forth between two adjacent phenyl groups, see (b) in Scheme 3.

(B). THF-Based 16-crown-4 (2). Considering these results, we moved to the cyclic THF-based 16-crown-4 structure **2**, see Scheme 2, as the organic template. The corresponding palladium derivative of **2** [(a) or (b) in Scheme 5] is similar to that of **1** but based on a ring with sp^3 carbon atoms, which are more prone to be involved in the Pd/H rearrangements that we are looking for. Thus, **2** should allow the palladium atom to roll throughout the structure in a sequence made of successive [1,5 + 1,2] Pd/H rearrangements, as shown, for instance, for the anticlockwise rotation depicted in Scheme 5 [see (a)].

There are eight possible isomers for the palladated form of **2** taking into account (i) the position of the metallic moiety with respect to the macrocycle, with Pd bound either to carbon 1 or to carbon 2 which are not equivalent, see (c) in Scheme 5; (ii) whether Pd adopts an *endo* or an *exo* spatial disposition, and (iii) the position of Br with respect to the carbon directly attached to Pd −yielding either *cis* or *trans* isomers. An example corresponding to the *trans*-**2**-*exo2* isomer is given in (**b**) of Scheme 5.

Table 1. Calculated Energies (ΔE) and Enthalpies (ΔH) of the Eight Possible Isomers for the Palladated Structure of **2**[a,b]

system	ΔE	ΔH
trans-**2**-*exo1*	0.0	0.0
trans-**2**-*exo2*	−2.5	−2.5
trans-**2**-*endo1*	+5.4	+5.7
trans-**2**-*endo2*	+2.7	+3.3
cis-**2**-*exo1*	+0.3	−0.4
cis-**2**-*exo2*	−2.2	−2.8
cis-**2**-*endo1*	+10.2	+9.8
cis-**2**-*endo2*	+7.4	+7.5

[a] The values are in kcal mol^{-1}, the zero of energy has been referred to *trans*-**2**-*exo1*. [b] The B3LYP total energy (in a. u.) is for *trans*-**2**-*exo1*: $E = -1564.944735$, $H = -1564.391544$.

Table 2. Calculated Energies (ΔE) and Enthalpies (ΔH) for the Species Involved in the *trans*-**2**-*exo1* → *trans*-**2**-*exo2* Transformation[a,b]

system	ΔE	ΔH	imaginary frequency[c]
trans-**2**-*exo1*	0.0	0.0	
trans-**2**-*exo*-TS1	+10.3	+7.4	469*i*
trans-**2**-*exo*-inter1	+9.1	+7.1	
trans-**2**-*exo*-TS2	+9.5	+6.8	27*i*
trans-**2**-*exo*-inter2	+5.1	+3.2	
trans-**2**-*exo*-TS3	+9.7	+6.9	32*i*
trans-**2**-*exo*-inter3	+9.1	+6.9	
trans-**2**-*exo*-TS4	+10.2	+7.2	467*i*
trans-**2**-*exo2*	−2.5	−2.5	

[a] The values are in kcal mol^{-1}, the zero of energy for the Pd migration in **2** refers to *trans*-**2**-*exo1*. [b] The B3LYP total energy (in a. u.) is for *trans*-**2**-*exo1*: $E = -1564.944735$, $H = -1564.391544$. [c] In cm^{-1}, refers to the unique imaginary frequency of the calculated transition state.

The energy of these eight isomers varies within a margin of 13 kcal mol^{-1}, see Table 1. We will, for the sake of brevity, focus here on one *exo* and one *endo* isomer, namely, the *trans*-**2**-*exo1* and the *cis*-**2**-*endo1* isomer as representatives of the initial position for Pd. Note that the *endo* isomers are energetically disfavored: Since the metallic moiety is oriented toward the interior of the structure, the steric interactions between the palladium substituents and the ring are very much increased in these isomers compared to the *exo* isomers.

(B.1). 1,2 Pd/H Interchange. The 1,2 Pd/H interchange that leads from the *trans*-**2**-*exo1* isomer to the *trans*-**2**-*exo2* isomer appears, from our calculations, to be rather facile. Yet, the apparent simplicity of such a 1,2 Pd migration is misleading since, as analyzed previously,[20] this process involves several transient species that lie on a relatively complex and flat potential surface, with three intermediates and four transition states, see Table 2 and Figure 1.

One difference between the *trans*-**2**-*exo*-TS1 and *trans*-**2**-*exo*-TS4 transition states may be mentioned: while in *trans*-**2**-*exo*-TS1 the hydrogen atom being transferred is closer to the carbon moiety, in *trans*-**2**-*exo*-TS4 this hydrogen is closer to Pd. The energy difference between these two situations is, however, rather small: only 0.2 kcal mol^{-1} (Table 2). This is eventually in disagreement with the Hammond postulate. Note also the low imaginary frequencies found for *trans*-**2**-*exo*-TS2 and *trans*-**2**-*exo*-TS2 (as below

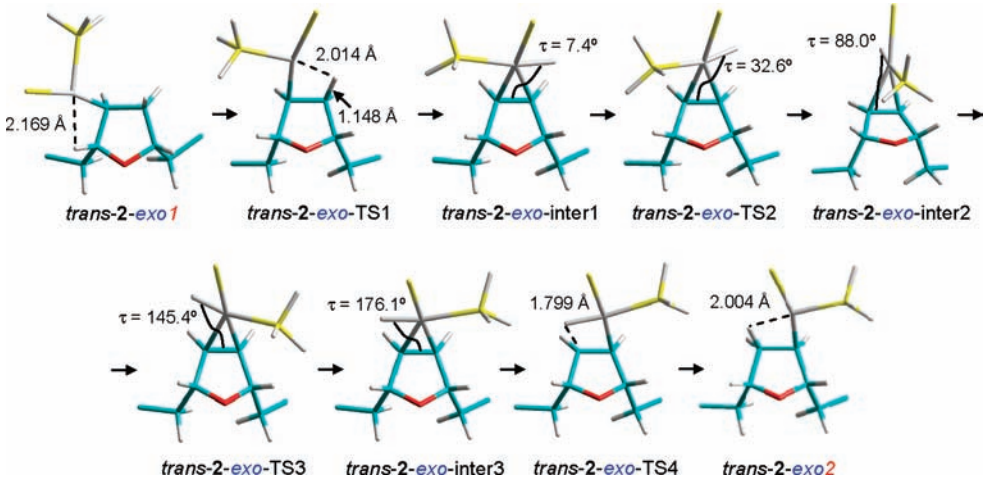

Figure 1. Mechanism of the 1,2 Pd migration from the *trans*-**2**-*exo1* isomer. Only one THF unit has been represented for clarity.

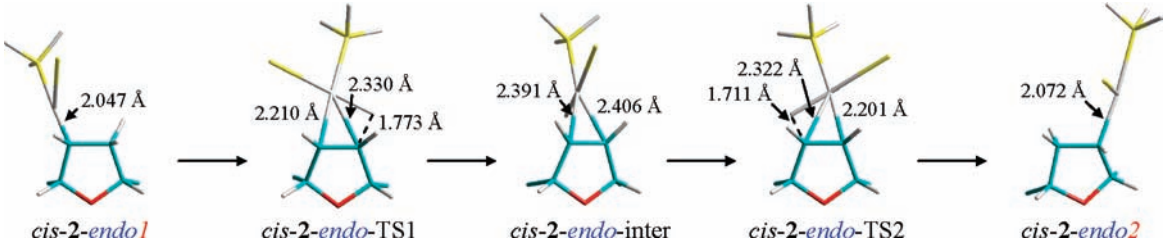

Figure 2. Mechanism of the 1,2 Pd migration from the *cis*-**2**-*endo1* isomer. Only one THF unit has been represented for clarity.

Table 3. Calculated Energies (ΔE) and Enthalpies (ΔH) for the Species Involved in the *cis*-**2**-*endo1* → *cis*-**2**-*endo2* Transformation[a,b]

system	ΔE	ΔH	imaginary frequency[c]
cis-**2**-*endo1*	0.0	0.0	
cis-**2**-*endo*-TS1	+10.4	+7.6	555*i*
cis-**2**-*endo*-inter	+0.6	−0.9	
cis-**2**-*endo*-TS2	+9.8	+7.1	657*i*
cis-**2**-*endo2*	−2.8	−2.3	

[a] The values are in kcal mol^{-1}, the zero of energy for the Pd migration in **2** refers to *cis*-**2**-*endo1*. [b] The B3LYP total energy (in a. u.) is for *cis*-**2**-*endo1*: $E = -1564.928448$, $H = -1564.375967$. [c] In cm^{-1}, refers to the unique imaginary frequency of the calculated transition state.

in Table 5 for *trans*-**3**-*endo*-TS2 and *trans*-**3**-*endo*-TS3). These frequencies correspond well to torsion displacements involving a big molecular mass as described in our previous work.[18−20]

We also looked for reasons that will be clear in the following, at the 1,2 Pd/H rearrangement from the *cis*-**2**-*endo1* structure. It leads to the *cis*-**2**-*endo2* structure, see Figure 2, following a pathway akin to the one calculated for *trans*-**2**-*exo1*, although the number of steps is reduced (see the Figure 2 and the Table 3). The barriers involved are quite similar to the ones found for the *trans*-**2**-*exo1* structure, and the energy required for the overall change remains rather moderate, 7.4 kcal mol^{-1} (enthalpy value). We have not computed other 1,2 Pd/H rearrangements that would take place on the top of the THF ring, such as the *cis*-**2**-*exo1*/*cis*-**2**-*exo2* and *trans*-**2**-*endo1*/*trans*-**2**-*endo2* rearrangements, but from this value and from the one found for the 1,2 shift starting from the *trans*-**2**-*exo1* structure one may reasonably conclude that such 1,2 shifts are rather easy.

The differences encountered between the 1,2-*exo* and 1,2-*endo* mechanisms can be attributed to the extremely flat potential surface exhibited by this kind of processes, making the involved torsional transition states (as *trans*-**2**-*exo*-TS2 or *trans*-**2**-*exo*-TS3) appear or not.

(B.2). 1,5 Pd/H Interchange. The situation is different for the rearrangement to be considered next, namely, the 1,5 Pd/H interchange between two adjacent THF rings. Note that, in contrast to the 1,2 rearrangement, this 1,5 Pd/H interchange interconverts *trans* isomers to *cis* ones and vice versa. Thus the *trans*-**2**-*exo2* structure will evolve to the *cis*-**2**-*exo1* isomer, see (a) in Scheme 6, and the *cis*-**2**-*exo2* isomer would lead to the *trans*-**2**-*exo1* isomer, see (b) in Scheme 6. The corresponding results are summarized in Table 4. They point to high enthalpy barriers for both *trans* and *cis* isomers, whatever the mechanism is, either a one step Pd(II) or a two-step Pd(IV). The Pd(II) and Pd(IV) pathways are shown in Figure 3 for the *trans*-**2**-*exo2* → *cis*-**2**-*exo1* rearrangement. That the Pd(II) pathway goes through a high energy transition state is at variance with our previous studies, where 1,5 Pd/H rearrangements were found to have barriers ranging between 28 and 36 kcal mol^{-1}.[18−20] It also differs from the results obtained for **1** (vide supra). We trace this feature to the fact that the corresponding transition state cannot easily attain the geometry required, that is, a more or less planar arrangement of the PdBr(PH_3) moiety and of the transferred hydrogen.[19] While the C−C distance between the carbon atoms involved in the Pd migration amounts to 3.611 Å in the transition state for the 1,5 shift in **1**, it amounts to 2.666 Å only, in the corresponding 1,5 transition state for **2**, thus introducing in the latter case a

Scheme 6. 1,5 Pd/H Interchange in the Palladated THF-Based 16-crown-4 Structure **2**: Geometric Considerations

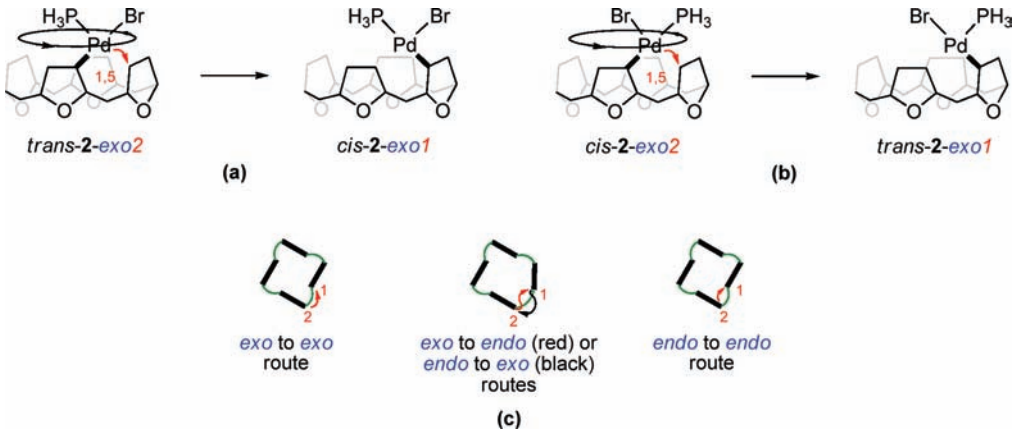

Table 4. Calculated Energies (ΔE) and Enthalpies (ΔH) for the Species Involved in the *trans*-**2**-*exo2* → *cis*-**2**-*exo1* and *trans*-**2**-*exo2* → *cis*-**2**-*endo1* Transformations[a,b]

	mechanism	system	ΔE	ΔH	imaginary frequency[c]
		exo to *exo*			
from *trans*-**2**-*exo2*	Pd(II)	*trans*-**2**-*exo2*	0.0	0.0	
		trans-**2**-*exo*-TS	+59.7	+57.0	1389*i*
		cis-**2**-*exo1*	+2.8	+2.2	
	Pd(IV)	*trans*-**2**-*exo2*	0.0	0.0	
		trans-**2**-*exo*-TSa	+51.5	+48.6	523*i*
		trans-**2**-*exo*-inter	+46.3	+44.8	
		trans-**2**-*exo*-TSb	+48.2	+45.4	366*i*
		cis-**2**-*exo1*	+2.8	+2.2	
from *cis*-**2**-*exo2*	Pd(II)	*cis*-**2**-*exo2*	0.0 (+0.3)[d]	0.0 (−0.3)[d]	
		cis-**2**-*exo*-TS	+59.3	+57.1	1390*i*
		trans-**2**-*exo1*	+2.2	+2.8	
	Pd(IV)	*cis*-**2**-*exo2*	0.0 (+0.3)[d]	0.0 (−0.3)[d]	
		cis-**2**-*exo*-TSa	+47.6	+45.5	402*i*
		cis-**2**-*exo*-inter	+45.7	+44.6	
		cis-**2**-*exo*-TSb	+50.9	+48.7	494*i*
		trans-**2**-*exo1*	+2.2	+2.8	
		endo to *endo*			
from *cis*-**2**-*endo2*	Pd(II)	*cis*-**2**-*endo2*	0.0 (+9.9)[d]	0.0 (+10.0)[d]	
		cis-**2**-*endo*-TS	+23.1	+20.2	1298*i*
		trans-**2**-*endo1*	−2.0	−1.8	
from *trans*-**2**-*endo2*	Pd(II)	*trans*-**2**-*endo2*	0.0 (+5.2)[d]	0.0 (+5.8)[d]	
		trans-**2**-*endo*-TS	+27.8	+24.6	1298*i*
		cis-**2**-*endo1*	+7.5	+6.5	
		exo to *endo*			
from *trans*-**2**-*exo2*	Pd(II)	*trans*-**2**-*exo2*	0.0	0.0	
		trans-**2**-*exo*-TSbis	+42.8	+40.0	1088*i*
		cis-**2**-*endo1*	+12.7	+12.3	

[a] The values are in kcal mol^{-1}, the zero of energy for the Pd migration in **2** refers to *trans*-**2**-*exo2*. [b] The B3LYP total energy (in a. u.) is for *trans*-**2**-*exo2*: E = −1564.948739, H = −1564.395595. [c] In cm^{-1}, refers to the unique imaginary frequency of the calculated transition state. [d] The values in parentheses refer to *trans*-**2**-*exo2*.

considerable strain energy. As a result, one gets very high activation barriers of ∼57 kcal mol^{-1}, see Table 4. The two-step Pd(IV) pathways are slightly more favorable, see Table 4, but with barriers which remain quite large, 48.6 kcal mol^{-1} for *trans*-**2**-*exo2* → *cis*-**2**-*exo1*, or 48.7 kcal mol^{-1} for *cis*-**2**-*exo2* → *trans*-**2**-*exo1* rearrangement (enthalpy values).

In contrast to the *exo* isomers, the *endo* isomers are characterized by 1,5 Pd/H rearrangement that are more facile, see Table 4. Thus, the *cis*-**2**-*endo2* → *trans*-**2**-*endo1* and *trans*-**2**-*endo2* → *cis*-**2**-*endo1* processes have barriers amounting to 20.2 and 24.6 kcal mol^{-1} (enthalpy values), respectively. The same is true of the corresponding reverse processes with barriers of 22.0 and 18.1 kcal mol^{-1}, respectively. The Pd migration can also be described as involving a Pd(II) mechanism. The energy barrier values are in the range of the values obtained for 1,5 rearrangements that we analyzed in previous work.[18−20] Note that in this case we could not find any Pd(IV) pathway. This is most likely due to the *endo* disposition: a hydride sitting at the apex of palladium, inside the core of the cyclomer, would suffer from severe steric repulsions.

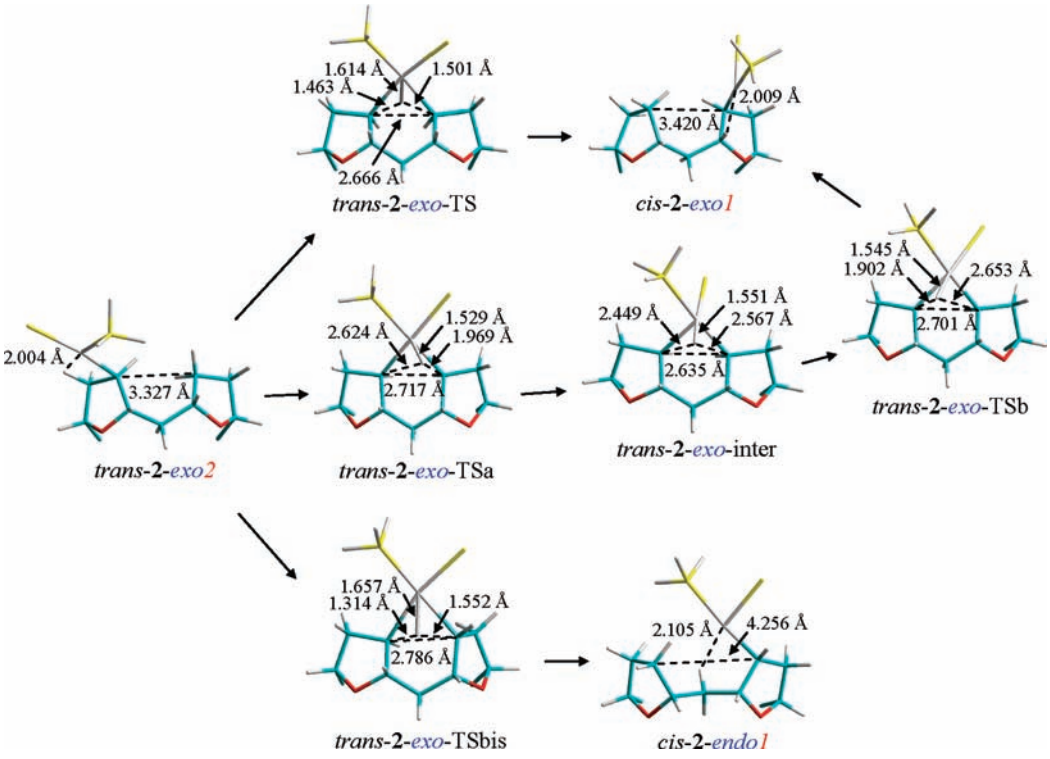

Figure 3. Mechanism of the 1,5 Pd migration from the *trans*-**2**-*exo2* isomer. Only two THF units have been represented for clarity.

Scheme 7. 1,5 Pd/H Interchange in the Palladated THF-Based 16-crown-4 Structure **2**

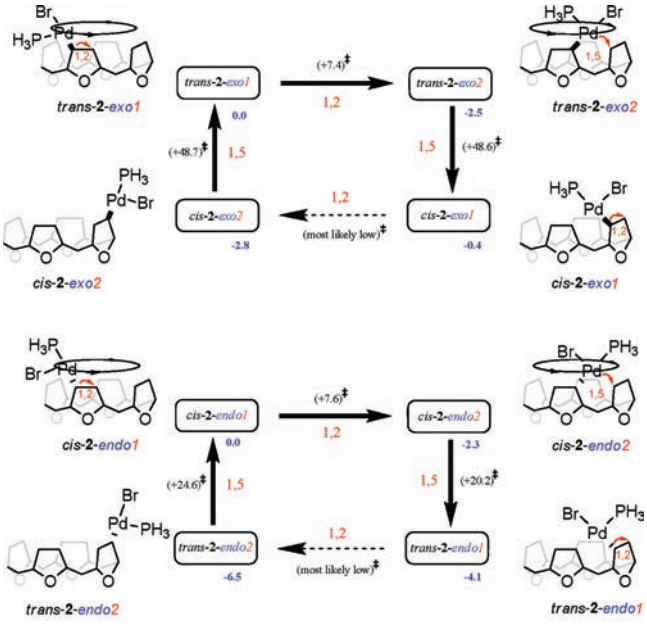

We finally consider an *exo* to *endo* Pd migration. For trans-**2**-*exo2* it would lead to the *cis*-**2**-*endo1*, see the Figure 3, but the corresponding barrier is again rather high, 40.0 kcal mol^{-1}. This particular process implies the deformation of the relatively rigid structure of C_4 symmetry [see (c) in Scheme 6] to accommodate the metallic moiety in the *endo* structure, hence leading to a relatively high energy Pd(II) transition state (Table 4). In this case, a Pd(IV) mechanism connecting both isomers could not be found.

Scheme 8. Possible Pathways from System *trans*-**3**-*endo1* [(**a**)], Geometric and Isomeric Considerations [(**b**) and (**c**)]

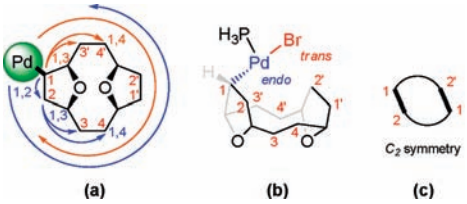

Table 5. Calculated Energies (ΔE) and Enthalpies (ΔH) for the Species Involved in the *trans*-**3**-*endo1* → *trans*-**3**-*endo2* Transformation[a,b]

system	ΔE	ΔH	imaginary frequency[c]
trans-**3**-*endo1*	0.0	0.0	
trans-**3**-*endo*-TS1	+13.4	+10.3	423*i*
trans-**3**-*endo*-inter1	+12.6	+10.4	
trans-**3**-*endo*-TS2	+15.9	+13.0	25*i*
trans-**3**-*endo*-inter2	+15.0	+12.7	
trans-**3**-*endo*-TS3	+15.1	+12.2	21*i*
trans-**3**-*endo*-inter3	+12.7	+10.5	
trans-**3**-*endo*-TS4	+13.6	+10.5	442*i*
trans-**3**-*endo2*	−1.5	−1.2	

[a] The values are in kcal mol^{-1}, the zero of energy for the Pd migration in **3** refers to *trans*-**3**-*endo1*. [b] The B3LYP total energy (in a. u.) is for *trans*-**3**-*endo1*: $E = -1102.455797$, $H = -1102.109102$. [c] In cm^{-1}, refers to the unique imaginary frequency of the calculated transition state.

(B.3). [1,2 + 1,5] Sequential Process. We are now in a position to discuss the feasibility of a [1,2 + 1,5] sequential process that would allow the metallic moiety to undergo an endless circular motion around the macrocycle. The two possibilities, either through an *exo* or through an *endo* structure are summarized in Scheme 7. Looking first at the *exo* structures, which are the most stable, see Table 1, it is clear that the high barriers computed for

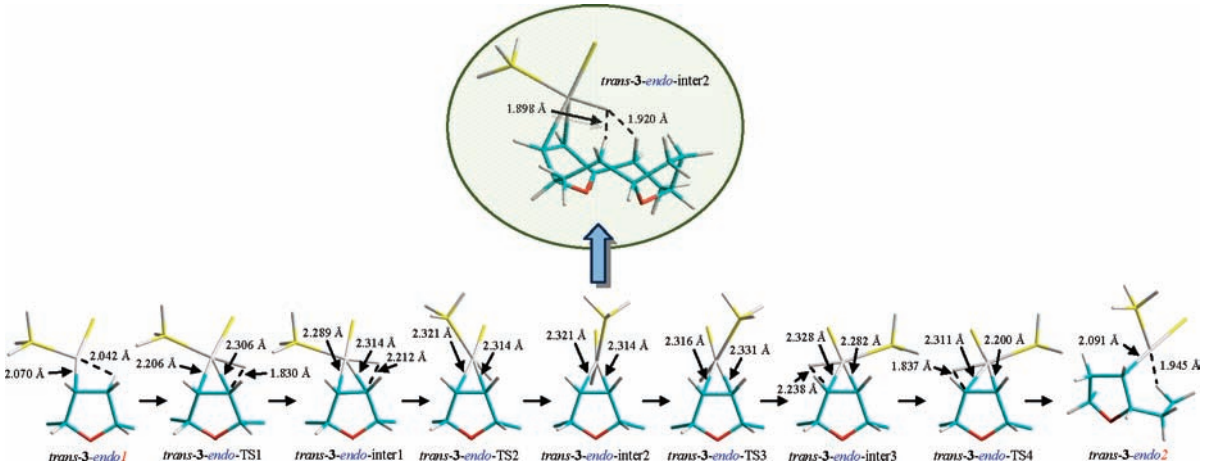

Figure 4. Mechanism of the 1,2 Pd migration from the *trans*-**3**-*endo1* isomer. Only one THF unit has been represented for clarity.

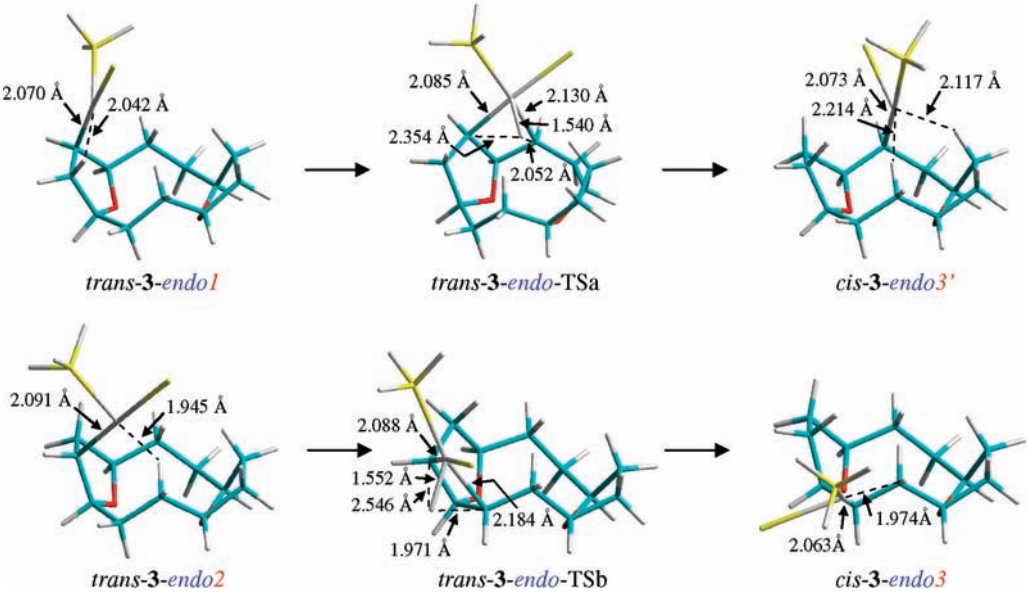

Figure 5. Mechanism of the 1,3 Pd migration from the *trans*-**3**-*endo1* and *trans*-**3**-*endo2* isomers.

Table 6. Calculated Energies (ΔE) and Enthalpies (ΔH) for the Species Involved in the *trans*-**3**-*endo1* → *cis*-**3**-*endo3′* Transformation[a,b,c]

system	ΔE	ΔH	imaginary frequency[d]
trans-**3**-*endo1*	0.0	0.0	
trans-**3**-*endo*-TSa	+41.2 (+38.9)[e]	+37.6 (+36.4)[e]	301*i* (337*i*)[e]
cis-**3**-*endo3′*	+6.5 (+7.0)[e]	+6.0 (+6.5)[e]	
trans-**3**-*endo2*	0.0	0.0	
trans-**3**-*endo*-TSb	+38.9	+35.4	424*i*
cis-**3**-*endo3*	−1.6	−2.2	

[a] The values are in kcal mol^{-1}, the zero of energy for the Pd migration in **3** refers, respectively, to *trans*-**3**-*endo1* and *trans*-**3**-*endo2*. [b] The B3LYP total energy (in a. u.) is for *trans*-**3**-*endo1*: $E = -1102.455797$, $H = -1102.109102$ (normal basis set); and $E = -1102.666326$, $H = -1102.322856$ (high basis set). [c] The B3LYP total energy (in a. u.) is for *trans*-**3**-*endo2*: $E = -1102.458256$, $H = -1102.110972$. [d] In cm^{-1}, refers to the unique imaginary frequency of the calculated transition state. [e] The value in parentheses refer to the use of the 6-311+G(d,p) basis set for C, H, and P atoms.

the *trans*-**2**-*exo2* → *cis*-**2**-*exo1* and *cis*-**2**-*exo2* → *trans*-**2**-*exo1* 1,5 rearrangements prohibit any circular motion.

Scheme 9. Possible 1,4 Pathways from Systems *trans*-**3**-*endo1* and *trans*-**3**-*endo2*

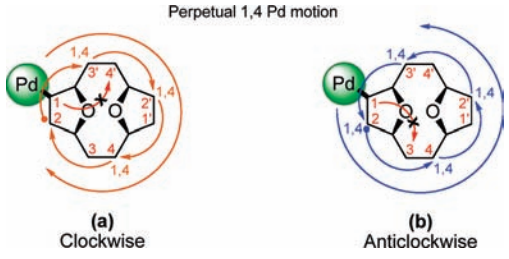

The system could only achieve back and forth 1,2 Pd/H interchanges between the 1 and 2 positions, either in its *trans* or in its *cis* form.

In contrast the barriers computed for the *cis*-**2**-*endo1* → *cis*-**2**-*endo2* 1,2 rearrangement and for the *cis*-**2**-*endo2* → *trans*-**2**-*endo1* and *trans*-**2**-*endo2* → *cis1*-**2**-*endo1* 1,5 Pd/H rearrangements point to the feasibility of a circular motion for the *endo* structures (see Scheme 7), the overall barrier being somewhat less than 25 kcal mol^{-1} in both directions. But one should recall that the *endo* structures

Table 7. Calculated Energies (ΔE) and Enthalpies (ΔH) for the Species Involved in the *trans*-**3**-*endo2* → *cis*-**3**-*endo4* and *cis*-**3**-*endo4* → *trans*-**3**-*endo2′* Transformations[a,b,c,d]

mechanism	system	ΔE	ΔH	imaginary frequency[e]
		1st Pd shift		
Pd(II) mechanism	*trans*-**3**-*endo2*	0.0	0.0	
	trans-**3**-*endo*-TS(II)	+37.8	+34.2	1389*i*
	cis-**3**-*endo4*	+8.0	+7.2	
Pd(IV) mechanism	*trans*-**3**-*endo2*	0.0	0.0	
	trans-**3**-*endo*-TS(IV)	+36.4	+32.7	432*i*
	cis-**3**-*endo4*	+8.0	+7.2	
		2nd Pd shift		
Pd(II) mechanism	*cis*-**3**-*endo4*	0.0	0.0	
	cis-**3**-*endo*-TS(II)	+37.4	+34.7	1401*i*
	trans-**3**-*endo2′*	−8.0	−7.2	
Pd(IV) mechanism	*cis*-**3**-*endo4*	0.0	0.0	
	cis-**3**-*endo*-TS(IV)	+36.2	+33.3	179*i*
	trans-**3**-*endo2′*	−8.0	−7.2	

[a] The values are in kcal mol^{-1}, the zero of energy for the Pd migration in **2** refers to *trans*-**2**-*exo2* for the first 1,4 Pd shift and to *cis*-**3**-*endo4* for the second 1,4 Pd shift. [b] The B3LYP total energy (in a. u.) is for *trans*-**3**-*endo2*: $E = -1102.458256$, $H = -1102.110972$. [c] The B3LYP total energy (in a. u.) is for *cis*-**3**-*endo4*: $E = -1102.445479$, $H = -1102.099567$. [d] Note that, owing to the C_2 symmetry of the macrocycle, *cis*-**3**-*endo4* is equivalent to the already mentioned *cis*-**3**-*endo3′*, and *trans*-**3**-*endo2′* equivalent to *trans*-**3**-*endo2*. [e] In cm^{-1}, refers to the unique imaginary frequency of the calculated transition state.

are less stable than the *exo* ones, see Table 1. For the *trans*-**2**-*exo2*/*cis*-**2**-*endo1* pair, the enthalpy difference is the highest, 12.3 kcal mol^{-1}. Moreover, we have seen that the enthalpy barrier for the *intramolecular exo* to *endo* pathway is large, 40 kcal mol^{-1} in the case of the *trans*-**2**-*exo2* → *cis*-**2**-*endo1* process. It would be therefore difficult to obtain an *endo* structure once an *exo* one has been synthesized. Note, however, that the reverse *cis*-**2**-*endo1* → *trans*-**2**-*exo2* process has a barrier (27.7 kcal mol^{-1}) that is somewhat higher than the barriers involved in the circular movement. Thus, should one be able to synthesize from the onset an *endo* structure, then a circular movement within the *endo* structure would be more facile than going back to the *exo* structure.

(C). THF-Ethylene Dimer (3). We finally modeled a third structure based on a THF-ethylene cyclic dimer (**3**). This structure should be more accessible for the *endo* positioning of the $PdBr(PH_3)$ moiety, and hence be potentially a good candidate for the rotation of this moiety. This motion can be achieved in several ways, either 1,2, 1,3 or 1,4, depending on the length of the through-space palladium displacement, (Scheme 8).

Indeed, the enthalpy difference between the *endo* and the *exo* structures is now quite small: The *trans*-**3**-*endo1* and *trans*-**3**-*endo2* structures are less stable than their *trans*-**3**-*exo1* and *trans*-**3**-*exo2* counterparts by 2.1 and 1.2 kcal mol^{-1} only, respectively. We will therefore restrict our discussion mainly to the *endo* structures. Note that the much higher enthalpy barriers computed for the 1,3 Pd/H rearrangement in the *exo* structure compared to the *endo* one, see below, also justifies this restriction. Thus, taking *trans*-**3**-*endo1* as the starting position, we first considered the 1,2 Pd/H rearrangement along one THF ring.

(C.1). 1,2 Pd Migration. This Pd/H rearrangement is shown in Figure 4 and the corresponding energetic parameters are reported in Table 5. They point to activation energies that are somewhat higher than the activation energies obtained in the previous 1,2 Pd/H rearrangement (by about 5 kcal mol^{-1}) and to a potential energy surface that is flatter, see Table 5. In particular, the central energy well that appeared in the energy profile computed for *trans*-**2**-*exo*-inter2 (Table 2) and, more distinctly, for *cis*-**2**-*endo*-inter (Table 3) is not observed here. This is due to the steric hindrance experienced by the transferred hydrogen, which points toward the hydrogen atoms of the methylene groups of the macrocycle. See for example the H···H close distances involved in the *trans*-**3**-*endo*-inter2 structure (up in Figure 4).

(C.2). 1,3 Pd Migration. As it can be depicted by (c) in Scheme 8, the symmetry of **3** is such that two possible 1,3 Pd/H rearrangements, see (a) in the same scheme, could be envisaged: (i) a metallic moiety displacement from *trans*-**3**-*endo1* to an "up" methylene of the chain (the 3′ position shown by (b) in Scheme 8) following a clockwise sense; (ii) a metallic moiety displacement from *trans*-**3**-*endo2* to a "down" methylene of the chain (the 3 position, see (b) in Scheme 8). This anticlockwise 1,3 migration would take place after the 1,2 Pd/H rearrangement between positions 1 and 2.

In both cases, the transition states for this 1,3 migration, shown in Figure 5, are relatively high in energy (about 38 and 35 kcal mol^{-1} above the starting structure, respectively, see Table 6), and of Pd(IV) type. As mentioned in the Computational Section, we checked whether the larger basis set [made of the 6-311+G(d,p) basis for the atoms other than Pd and Br] would change this value noticeably. As shown in Table 5, and in line with previous results,[18] this is not the case. That would mean that the results we have obtained for such processes along this work are significantly appropriate, at least concerning the basis set level used.

Note also that the barriers obtained for these 1,3 Pd shifts operating from either *trans*-**3**-*endo2* or *trans*-**3**-*endo1* are somewhat lower than the ones we obtained previously for the 1,3 Pd migration between the two phenyl rings of naphthalene (+46.6 kcal mol^{-1}).[19] They are also much lower than the barriers computed for the corresponding *exo* structures, for example, 59.2 kcal mol^{-1} (ΔH value) for the *trans*-**3**-*exo2* → *cis*-**3**-*exo3* rearrangement.

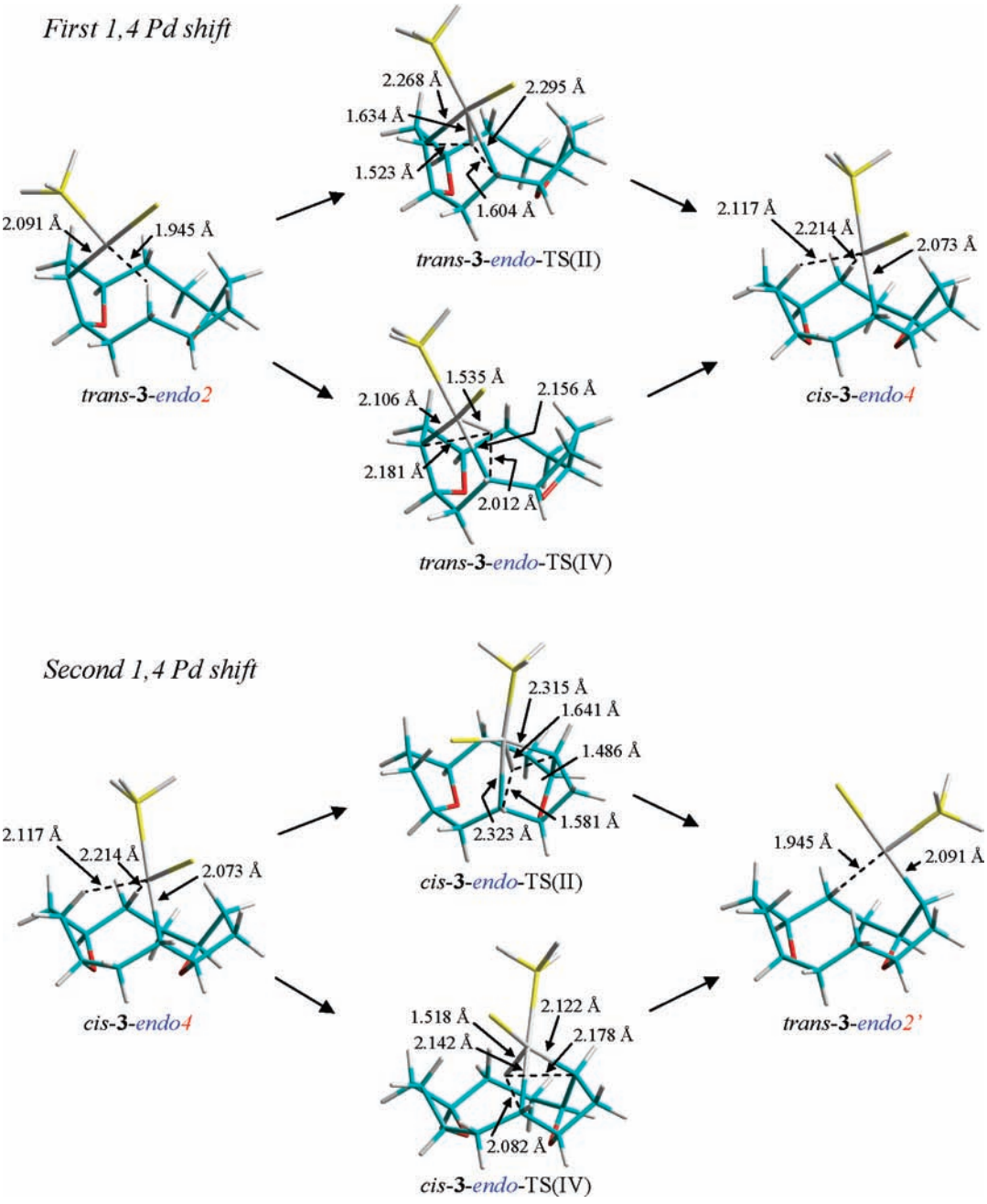

Figure 6. Pd(II) and Pd(IV) mechanisms of the linked 1,4 Pd migration from *trans*-**3**-*endo2*.

(**C.3**). **1,4 Pd Migration.** A thorough analysis of this process is important since for this system a series of four linked 1,4 Pd shifts should allow an endless motion of the Pd atom, see Scheme 9. There are, a priori, several possibilities to achieve this motion, depending on the starting position and on whether the motion is clockwise or anticlockwise. Yet the geometry of **3** is such that some of the pathways cannot be operative because of geometrical factors. This is the case for the clockwise, (a) of Scheme 9, and the anticlockwise, (b) of Scheme 9, motions that start at the position 1, since as best seen from (b) in Scheme 8, the "down"-methylene positions 4′ and 3 are not accessible via 1,4 Pd shifts from the positions 1 and 1′, respectively. On the other hand the "up"-methylene positions 4 and 3′ are accessible via 1,4 Pd shifts from the positions 2 and 2′ and vice versa. As a consequence, once a 1,2 Pd shift from the position 1 has taken place, a motion starting from the position 2 could take place either clockwise or anticlockwise.[39]

At this stage one should also mention that, owing to the C_2 symmetry of the macrocycle, carbon 1 and carbon 2 are not equivalent. They are, however, equivalent to 1′ and 2′, see (c) in Scheme 8. There are, therefore, small energy differences between the two different 1,4 Pd migrations starting either from *trans*-**3**-*endo1* or from *trans*-**3**-*endo2*.

(39) Although the Pd-fragment could probably go back and forth many times before performing a complete round, we suppose that, in the gas phase, the motion could be performed either clockwise or anticlockwise since the Pd-moving should continue following a defined direction impelled by the own moment of inertia.

Scheme 10. Enthalpy Profile for the Possible Mixed Pathways Occurring for a Clockwise and an Anticlockwise Pd Motion from *trans*-**3**-*endo2* to *trans*-**3**-*endo2′*

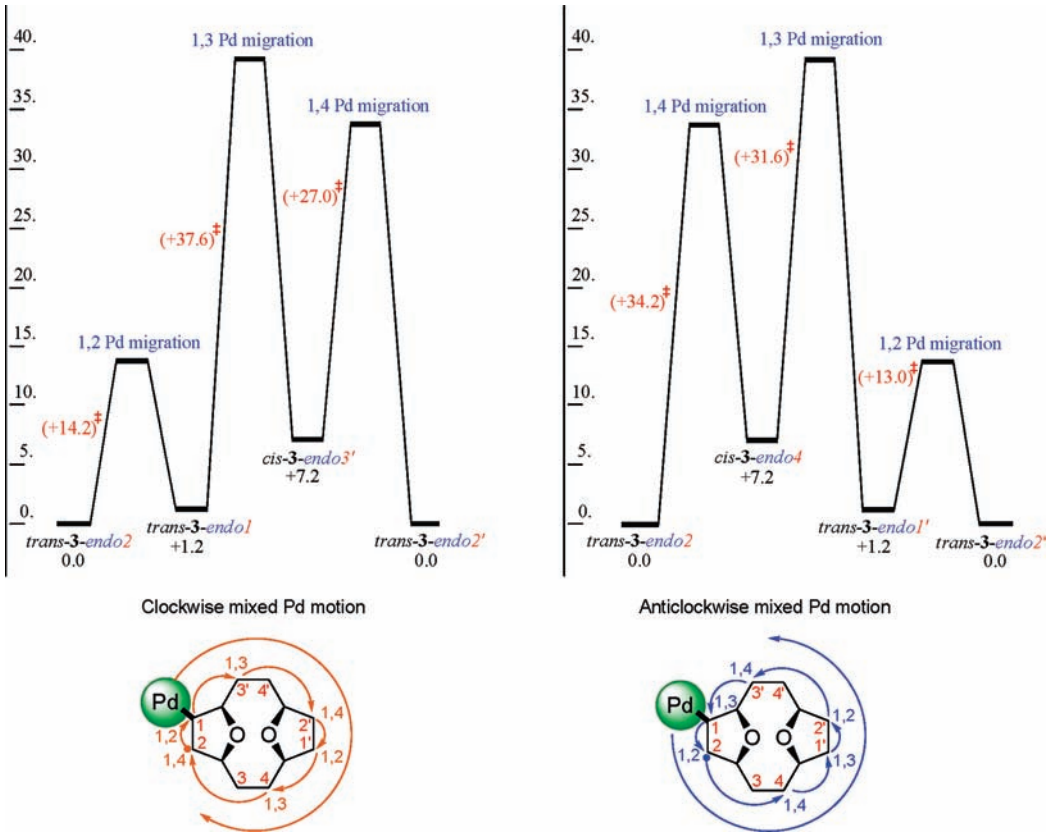

Moreover, one should note that the 2 → 4 and 4 → 2′ Pd/H interchanges are not equivalent either. Thus, for a full tour around the structure **3**, one needs to consider two different 1,4 Pd shifts, a first one between *trans*-**3**-*endo2* and *cis*-**3**-*endo4*, and a second one between *cis*-**3**-*endo4* and *trans*-**3**-*endo2′*. Then, the *trans*-**3**-*endo2′* → *cis*-**3**-*endo4′* and *cis*-**3**-*endo4′* → *trans*-**3**-*endo2* Pd/H interchanges that will complete the circular movement are just the equivalent of the two previous ones.

As shown in Table 7 and Figure 6 both *trans*-**3**-*endo2* → *cis*-**3**-*endo4* and *cis*-**3**-*endo4* → *trans*-**3**-*endo2′* can proceed via either Pd(II) or Pd(IV) transition states. This agrees with our previous results, which also underlined the possibility of Pd(II) and Pd(IV) competing mechanisms for such 1,4 transformations.[19,20] Here too, the two mechanisms have similar activation enthalpy values, the Pd(IV) route being slightly more favorable by about 1.5 kcal mol^{-1}, see Table 7.

One should notice that because of the destabilization of *cis*-**3**-*endo4* structure with respect to *trans*-**3**-*endo2* (by 7.2 kcal mol^{-1}), the highest point on the reaction path made of these successive 1,4 Pd/H interchanges corresponds to the *cis*-**3**-*endo4* → *trans*-**3**-*endo2′* step. The *cis*-**3**-endo-TS(IV) lies therefore 40.5 kcal mol^{-1} above *trans*-**3**-*endo2* and *trans*-**3**-*endo2′*. This feature severely affects the process. In fact, a sequence made of clockwise 1,2 + 1,3 + 1,4 + 1,2 + 1,3 + 1,4 shifts or anticlockwise 1,4 + 1,3 + 1,2 + 1,4 + 1,3 +1,2 shifts from *trans*-**3**-*endo2* instead of a 1,4 + 1,4 +1,4 +1,4 sequence, would become slightly preferable, the 1,3 Pd migration having a somewhat lower transition state, at 38.8 kcal mol^{-1} above *trans*-**3**-*endo2* and *trans*-**3**-*endo2′* see Scheme 10.[40] Such a conclusion was not expected on the basis of our previous calculations of 1,3 and 1,4 rearrangements in systems that are not cyclomeric.[19,20]

Final Remarks and Conclusion

We are now in a position to compare these three model structures, and more specifically the THF-based structures **2** and **3**, since the [1,1,1,1]paracyclophane system **1** turned out not to be a good candidate for a circular motion of the metallic moiety because of the very high barrier of the 1,2 Pd/H rearrangement within the phenyl ring. We traced this feature to the coplanarity, imposed by the sp^2 hybridation of the carbon atoms, of the two exchanging units, hydrogen on one carbon end, Pd(PH$_3$)Br on the other carbon end. On the other hand, as expected from our previous results, since the 1,5 Pd/H rearrangement appears to be rather facile, a pendulum movement of the metallic moeity between two adjacent phenyl groups could occur.

The THF-based systems **2** and **3** are free from the geometric constraint on the 1,2 shift imposed by the sp^2 carbon atoms that are bound to each other. They also offer more possibilities for the metallic moiety motion, owing, among other things, to the high number of geometric isomers that can be considered. For both systems, however, the *exo* to *exo* process appears to involve rather high barriers. On the other hand, *endo* to *endo* processes along the more sterically

(40) Owing to the C_2 symmetry of the macrocycle scaffold, the 1,3 transition state that needs to be considered here corresponds to *trans*-**3**-*endo*-TSa, see Table 5.

hindered *endo* face seem to be easier. For **2** an endless motion made of successive 1,2 and 1,5 shifts is characterized by barriers somewhat less than 30 kcal mol^{-1}. One shortcoming, however, is that the *endo* isomers should be difficult to obtain because of their destabilization with respect to the *exo* isomers and the very high barrier associated to the 1,2 *exo* to *endo* Pd/H interchange. **3** with its more opened structure was designed to remove this drawback. The *endo* structures are indeed more accessible. Yet the higher activation enthalpies associated to the 1,3 and 1,4 Pd/H interchanges compared to the 1,5 Pd/H interchange lead to energy differences between the lowest energy minimum and the highest transition state that are greater in **3**. Thus **2** should be a better candidate if one would be able to trap an *endo* structure.

Finally, one should mention that the possibility to set up a turning moiety also leads to the possibility of transmitting a signal each time that a pointer atom crosses through a particular position on the structure. This might allow the construction of molecular switches or molecular clocks. We now work on these aspects.

Acknowledgment. The calculations have been carried out at the Institut du Développement et des Ressources en Informatique Scientifique (IDRIS, Orsay, France) and at the Centro de Supercomputación de la Universidad de Granada (UGRGRID-CSIRC, Granada, Spain). We thank IDRIS and the Universidad de Granada for financial support.

Supporting Information Available: Complete reference 32, Cartesian coordinates, and intrinsic energies for all the calculated structures. This material is available free of charge via the Internet at http://pubs.acs.org.